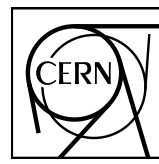


EUROPEAN ORGANIZATION FOR NUCLEAR RESEARCH



ALICE



CERN-PH-EP-2015-327

18 December 2015

Multi-strange baryon production in p–Pb collisions at $\sqrt{s_{\text{NN}}} = 5.02 \text{ TeV}$

ALICE Collaboration*

Abstract

The multi-strange baryon yields in Pb–Pb collisions have been shown to exhibit an enhancement relative to pp reactions. In this work, Ξ and Ω production rates have been measured with the ALICE detector as a function of transverse momentum, p_T , in p–Pb collisions at a centre-of-mass energy of $\sqrt{s_{\text{NN}}} = 5.02 \text{ TeV}$. The results cover the kinematic ranges $0.6 \text{ GeV}/c < p_T < 7.2 \text{ GeV}/c$ and $0.8 \text{ GeV}/c < p_T < 5 \text{ GeV}/c$, for Ξ and Ω respectively, in the common rapidity interval $-0.5 < y_{\text{CMS}} < 0$. Multi-strange baryons have been identified by reconstructing their weak decays into charged particles. The p_T spectra are analysed as a function of event charged-particle multiplicity, which in p–Pb collisions ranges over one order of magnitude and lies between those observed in pp and Pb–Pb collisions. The measured p_T distributions are compared to the expectations from a Blast-Wave model. The parameters which describe the production of lighter hadron species also describe the hyperon spectra in high multiplicity p–Pb collisions. The yield of hyperons relative to charged pions is studied and compared with results from pp and Pb–Pb collisions. A statistical model is employed, which describes the change in the ratios with volume using a canonical suppression mechanism, in which the small volume causes a species-dependent relative reduction of hadron production. The calculations, in which the magnitude of the effect depends on the strangeness content, show good qualitative agreement with the data.

© 2015 CERN for the benefit of the ALICE Collaboration.

Reproduction of this article or parts of it is allowed as specified in the CC-BY-4.0 license.

*See Appendix A for the list of collaboration members

1 Introduction

Collisions of heavy nuclei at ultra-relativistic energies allow the study of a deconfined state of matter, the Quark-Gluon Plasma, in which the degrees of freedom are partonic, rather than hadronic. The role of strange hadron yields in searching for this state was pointed out at an early stage [1]. It was subsequently found that in high energy nucleus-nucleus (A–A) collisions at the Super Proton Synchrotron (SPS), the Relativistic Heavy Ion Collider (RHIC) and the Large Hadron Collider (LHC) the abundances of strange and multi-strange baryons are compatible with those from thermal statistical model calculations [2–10].

In smaller collision systems at the same centre-of-mass energies, in particular proton-proton (pp) collisions, the relative abundance of multi-strange baryons is lower with respect to A–A collisions, whether normalised to participant nucleons or produced particles (pions or charged hadrons). This led to the interpretation that strangeness enhancement is observed in A–A collisions. Attempts to explain this phenomenon include the application of a canonical formalism in the statistical model, replacing the grand canonical approach, in which the requirement to conserve the strangeness quantum number when producing (multi-)strange baryons in small systems is imposed [11]. This means that strange hadrons are produced with a lower relative abundance in small systems, an effect known as canonical suppression. Such a theoretical framework has been used to make predictions for LHC energies [12]. Further complications in the interpretation arise when the produced system, although small, is formed in peripheral A–A collisions where the particle production may not be from a contiguous volume due to core-corona effects [13, 14]. Evidence for this effect was seen at RHIC where a canonical suppression calculation based on the estimated number of participant nucleons could not successfully reproduce the data [15]. A cleaner way to investigate canonical suppression effects is provided by proton–nucleus (p–A) collisions.

Proton–nucleus collisions provide an opportunity to study the p_{T} -dependence of the particle spectra created in a system with a different, more compact, initial geometry than A–A collisions where a similar number of charged particles are produced. Studying this dependence is important in determining the applicability of hydrodynamics [16] which has been successful in describing the particle spectra in A–A collisions [17–19].

At the LHC the combination of the rise in particle production per nucleon-nucleon collision with increasing \sqrt{s} and a dedicated p–Pb data-taking period have enabled the ALICE experiment to collect a large sample of Ξ^{\pm} and Ω^{\pm} . In this Letter, we set out the methods for these studies, present the results obtained and discuss how they fit into a theoretical picture.

2 Sample and data analysis

The results presented in this Letter were obtained from a sample of the data collected with the ALICE detector [20] during the LHC p–Pb run at $\sqrt{s_{\text{NN}}} = 5.02$ TeV in the beginning of 2013. The two scintillator arrays V0A (direction of Pb beam), and V0C (direction of p beam), covering pseudo-rapidity ranges of $2.8 < \eta < 5.1$ and $-3.7 < \eta < -1.7$, respectively, served both as triggering detectors and for determining the event multiplicity class [21]. The tracking of particles in the central barrel, covering $|\eta| < 0.9$, takes place in the Inner Tracking System (ITS), which consists of the two innermost silicon pixel layers, surrounded by two silicon drift and two silicon strip layers, all placed within a radius of 43 cm, and the Time Projection Chamber (TPC), a large cylindrical drift chamber filled with a Ne-CO₂ gas mixture [20]. Measurements of the energy loss by charged particles in the gas allow particles to be identified with this detector.

A trigger requiring a coincidence within less than 1 ns in the V0 detectors selected around 100 million events, which are mainly non-single diffractive (NSD) events and contain a negligible contribution from single diffractive (SD) and electromagnetic (EM) processes [22]. A dedicated radiator-quartz detector (T0) provided a measurement of the event time of the collisions. The V0 and T0 time resolutions allowed

discrimination of beam-beam interactions from background events in the interaction region. Further background suppression was applied in the offline analysis using time information from two neutron Zero Degree Calorimeters (ZDC), as was performed in previous p–Pb analyses [23]. Primary vertices (PVs) were selected if their position along the beam axis was reconstructed within 10 cm of the geometrical centre of the detector. In Monte Carlo (MC) studies an efficiency of 99.2% for this trigger was obtained, while the joint trigger and primary vertex reconstruction efficiency lies at 97.8% [22]. The estimated mean number of interactions per bunch crossing was below 1% in the sample chosen for this analysis.

The analysed events were divided into seven multiplicity percentile classes according to the total number of particles measured in the forward V0A detector. The efficiency-corrected mean number of charged primary particles per unit rapidity ($\langle dN_{\text{ch}}/d\eta \rangle$) within $-0.5 < \eta < 0.5$ in the laboratory reference frame for each of these multiplicity bins were published in [23].

Due to the asymmetric energies of the proton and lead ion beams, a consequence of the 2-in-1 magnet design of the LHC, the nucleon-nucleon centre-of-mass system is shifted by 0.465 units of rapidity in the direction of the proton beam with respect to the laboratory frame. The measurements reported in this Letter were performed in the central rapidity window defined in the centre-of-mass frame within $-0.5 < y < 0$, where negative rapidity corresponds to the side of the detector into which the Pb beam travels.

The identification of multi-strange baryons was based on the topology of their weak decays through the reconstruction of the tracks left behind by the decay products, referred to as the daughter particles. The daughters of the $\Xi^- \rightarrow \Lambda\pi^-$ (BR: 99.9%), $\Omega^- \rightarrow \Lambda K^-$ (BR: 67.8%) and the subsequent $\Lambda \rightarrow p\pi^-$ (BR: 63.9%) weak decays [24], as well as the corresponding decays of the $\bar{\Xi}^+$ and $\bar{\Omega}^+$, were reconstructed by combining track information from the TPC and the ITS [25]. Proton, anti-proton and charged π and K tracks were identified in the TPC via their measured energy deposition, which was compared with a mass-dependent parameterisation of ionisation loss in the TPC gas as a function of momentum [26]. All daughter candidates were required to lie within 4σ of their characteristic Bethe-Bloch energy loss curve. Multi-strange candidates were selected through the geometrical association of the V^0 component (Λ or $\bar{\Lambda}$ decay) to a further secondary, ‘bachelor’ track (identified as π^\pm or K^\pm). In this process, several geometrical variables were measured for each candidate, and criteria were set on them in order to purify the selected sample: numerical values for the selection cuts applied are reported in Table 1. These selections are similar to those in the pp measurements [25], a consequence of the low multiplicities present in the detector in the p–Pb collisions. As a result the correction factors for the efficiency are also similar. In addition to the settings on topological variables, a cut has been applied on the V^0 invariant mass window of ± 8 MeV/ c^2 from the nominal Λ mass [24]. Further restrictions were set on the proper lifetime of the Ξ^\pm and Ω^\pm . By requiring this variable to be less than 3 times the mean decay length (4.91 cm and 2.46 cm, respectively), we discarded low-momentum secondary particles and false multi-strange candidates, the daughter tracks of which originated from interactions with detector material.

The invariant mass of the Ξ and Ω hyperons was calculated by assuming the known masses [24] of the Λ and of the bachelor track. The mass was reconstructed twice for each cascade candidate, once assuming the bachelor to be a π and once a K . This allowed the removal of an important fraction of the Ω background, which contained a large contribution from the Ξ candidates that pass the Ω selection criteria. Most of these false Ω were removed discarding all candidates that could be reconstructed as Ξ with a mass within 10 MeV/ c^2 of the known mass [24] of the Ξ baryon. Figure 1 shows the invariant mass distributions for the Ξ^- and Ω^- hadrons in well populated p_T bins for the lowest and highest multiplicity classes.

For the signal extraction, a peak region was defined within 4σ of the mean of a Gaussian invariant mass peak for every measured p_T interval. Adjacent background bands, covering an equal combined mass interval as the peak region, were defined on both sides of that central region. This is illustrated in Figure

V^0 finding criteria	
<i>DCA: h^\pm to PV</i>	> 0.04 (0.03) cm
<i>DCA: h^- to h^+</i>	< 1.5 standard deviations
Δ mass (m_{V^0})	$1.108 < m_{V^0} < 1.124 \text{ GeV}/c^2$
<i>Fiducial volume (R_{2D})</i>	$R_{2D} > 1.1$ (1.2) cm
<i>V^0 pointing angle</i>	$\cos \theta_{V^0} > 0.97$

Cascade finding criteria	
<i>Proper decay length</i>	$< 3 \times$ mean decay length
<i>DCA: π^\pm (K^\pm) to PV</i>	> 0.04 cm
<i>DCA: V^0 to PV</i>	> 0.06 cm
<i>DCA: π^\pm (K^\pm) to V^0</i>	< 1.3 cm
<i>Fiducial volume (R_{2D})</i>	$R_{2D} > 0.5$ (0.6) cm
<i>Cascade pointing angle</i>	$\cos \theta_{\text{casc}} > 0.97$

Table 1: The parameters for V^0 (Λ and $\bar{\Lambda}$) and cascades (Ξ^\pm and Ω^\pm) selection criteria. Where a criterion for Ξ^\pm and Ω^\pm finding differs, the value for the Ω^\pm case is in parentheses. DCA represents “distance of closest approach,” PV the primary vertex, θ is the angle between the momentum vector of the reconstructed V^0 or cascade, and the displacement vector between the decay and primary vertices. The curvature of the cascade particle’s trajectory is neglected.

1 with the shaded bands on either side of the peak. The number of bin entries inside the side-bands was subtracted from the number of candidates within the peak region, assuming the background to be linear across the mass range considered.

The p_T distributions were corrected for detector acceptance and reconstruction efficiencies. These were estimated with the use of DPMJet [27] simulated Monte Carlo (MC) events, which were propagated through the detector with GEANT3 [28].

2.1 Systematic uncertainties

Systematic uncertainties due to the choice of selection criteria were examined separately in each p_T interval of the measured spectra. Individual settings were loosened and tightened, in order to measure changes in the signal loss correction. For the Ξ hyperons, the signal extraction accounts for an uncertainty of around 2% but reaches 5% at low- p_T and in high multiplicity events, while for the Ω , uncertainties of 3-5% were measured. The uncertainty due to the topological selections is around 2(3)% for the main p_T region, and up to 3(5)% at low momentum for $\Xi(\Omega)$. The constraint on the V^0 mass window contributes to the total uncertainty with around 0.5(1)% and both the TPC tracking and identification cuts with 2(3)%. The proper decay length cut gives another 3(5)% uncertainty at low p_T . A 4% error was added due to the material budget, and for the Ω^\pm only, an additional 3% due to the mass hypothesis cut. All these individual error contributions, which are listed in Table 2, are added in quadrature. Apart from the low momentum region, no p_T dependence is observed in the total uncertainty. The total systematic error lies between 5-6(8)% across the whole spectrum, reaching up to 8(14)% in the lowest p_T bins for the $\Xi(\Omega)$ baryons.

The fraction of the systematic error that is uncorrelated across multiplicity was calculated by using the same method applied in [23], in which spectra deviations in specific multiplicity classes were compared to those observed in the integrated data sample. The choice of the topological parameter values and the applied signal extraction method generates the dominant contribution to the uncorrelated uncertainties across multiplicity. These uncertainties were measured to be within 2% in the case of the Ξ and 3% in the case of the Ω , which constitutes a fraction that lies between 20 and 40% of the total systematic

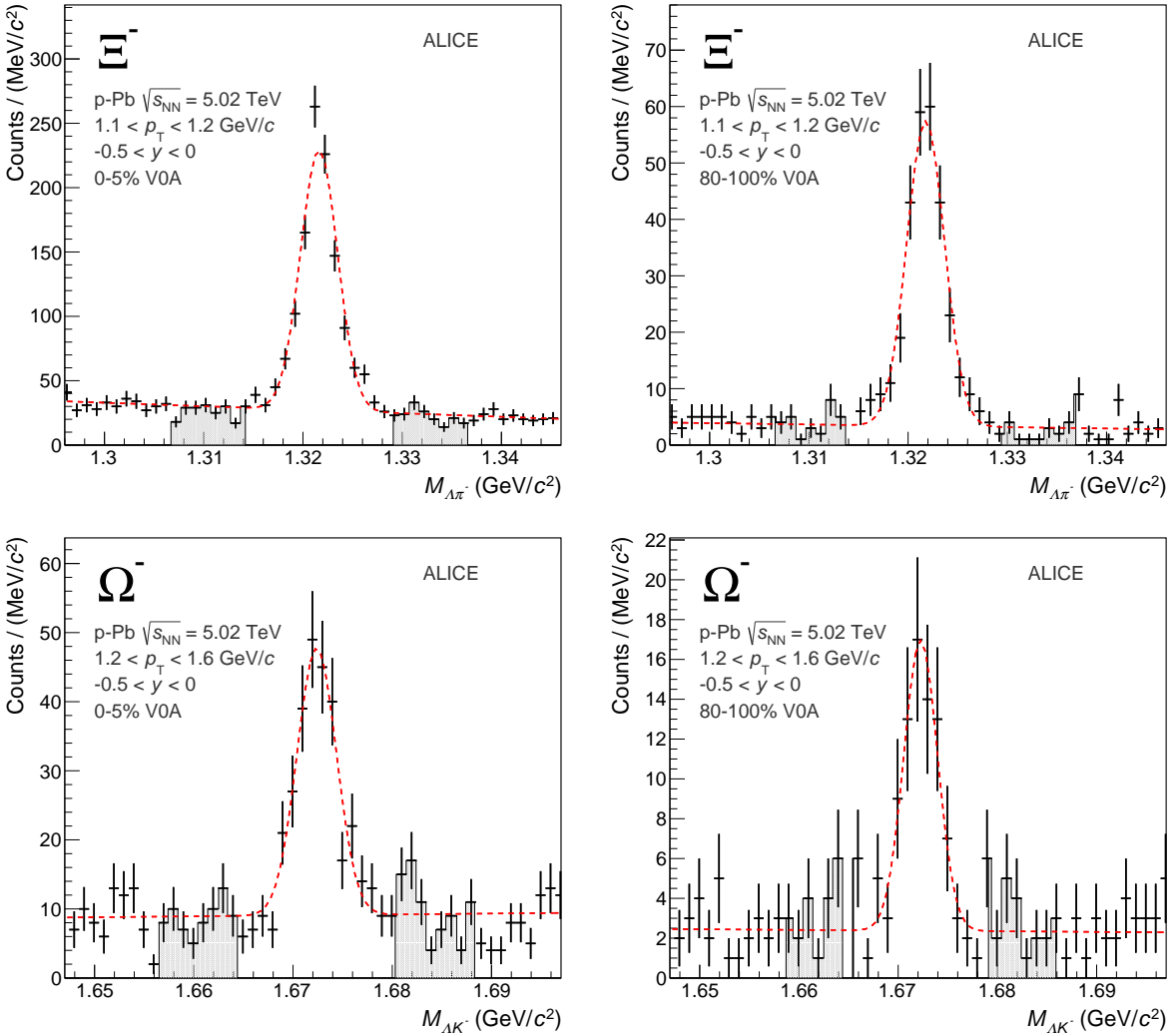


Fig. 1: Invariant mass distributions of the Ξ^- and Ω^- in the 1.1 - 1.2 GeV/c and 1.2 - 1.6 GeV/c p_{T} bins respectively, fitted with a Gaussian peak and linear background (dashed red curves). The distributions for highest (left) and lowest (right) multiplicity classes are shown. The fits only serve to illustrate the peak position with respect to which the bands were defined and the linear background assumption for the applied signal extraction method.

uncertainties.

3 Results

3.1 Transverse momentum spectra

The p_{T} distributions of Ξ^- , Ξ^+ , Ω^- and Ω^+ in $-0.5 < y < 0$ are shown in Fig. 2 for different multiplicity intervals, as defined in [23]. Since antiparticle and particle spectra are identical within uncertainties, the average of the two is shown. The spectra exhibit a progressive flattening with increasing multiplicity, which is qualitatively reminiscent of what is observed in Pb–Pb [10].

The calculation of p_{T} -integrated yields can be performed by using data in the measured region and a parametrisation-based extrapolation elsewhere. The Boltzmann-Gibbs Blast-Wave (BG-BW) model [16] gives a good description of each p_{T} spectrum and has been used as a tool for this extrapolation. Other alternatives, such as the Levy-Tsallis [29] and Boltzmann distributions, were used for estimating

Source	Ξ^\pm	Ω^\pm
Material budget	4%	4%
Competing mass hypothesis	-	3%
Topological variables	2-3(5)%	3-5%
Signal extraction	2(5)%	3(5)%
Particle identification	2%	3%
Track selection	2%	3%
Proper decay length	1(3)%	2(5)%
V^0 mass window	0.5%	1%

Table 2: Contributions to the total systematic uncertainties for the Ξ^\pm and Ω^\pm spectra measurements. The values in brackets indicate the maximum uncertainties measured for low p_T cascades (see text).

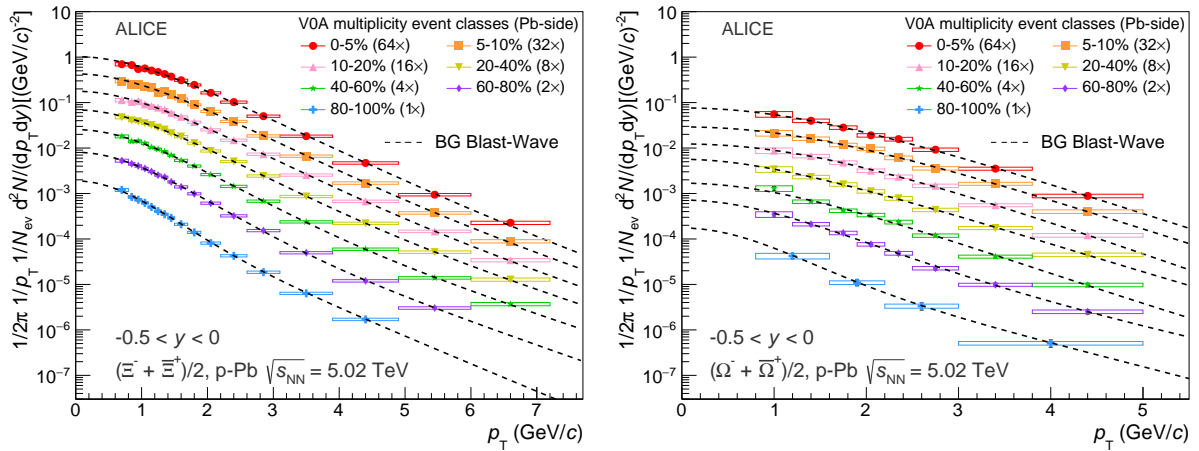


Fig. 2: (colour online) Invariant p_T -differential yields of $(\Xi^- + \Xi^+)$ and $(\Omega^- + \Omega^+)$ in different multiplicity classes. Data have been scaled by successive factors of 2 for better visibility. Statistical (bars), full systematic (boxes) and uncorrelated across multiplicity (transparent boxes) uncertainties are plotted. The dashed curves represent Blast-Wave fits to each individual distribution.

the systematic uncertainty due to the extrapolation.

The extrapolation in the unmeasured Ξ^\pm (Ω^\pm) low- p_T region grows progressively with decreasing multiplicity bins, from around 16%(19%) of the total yield in the 0–5% multiplicity class to around 27%(40%) in the 80–100% class. The systematic uncertainty assigned to the yield due to the extrapolation technique is 2.8%(7.8%) for high multiplicities and rises to 5.2%(14.5%) in the case where the fraction of the extrapolated yield is highest.

3.2 Comparison to Blast-Wave model

In order to investigate whether the observed spectral shapes are consistent with a system that exhibits hydrodynamical radial expansion, the measured distributions have been further studied in the context of the BG-BW model [16]. This model assumes a locally thermalised medium that expands collectively with a common velocity field and then undergoes an instantaneous freeze-out. In this framework, a simultaneous fit to identified particle spectra allows for the determination of common freeze-out parameters. These can be used to predict the p_T distribution for other particle species in a collective expansion picture. It should be noted that such a simultaneous fit differs from the individual fits mentioned in the previous section and used only for extrapolating the spectra.

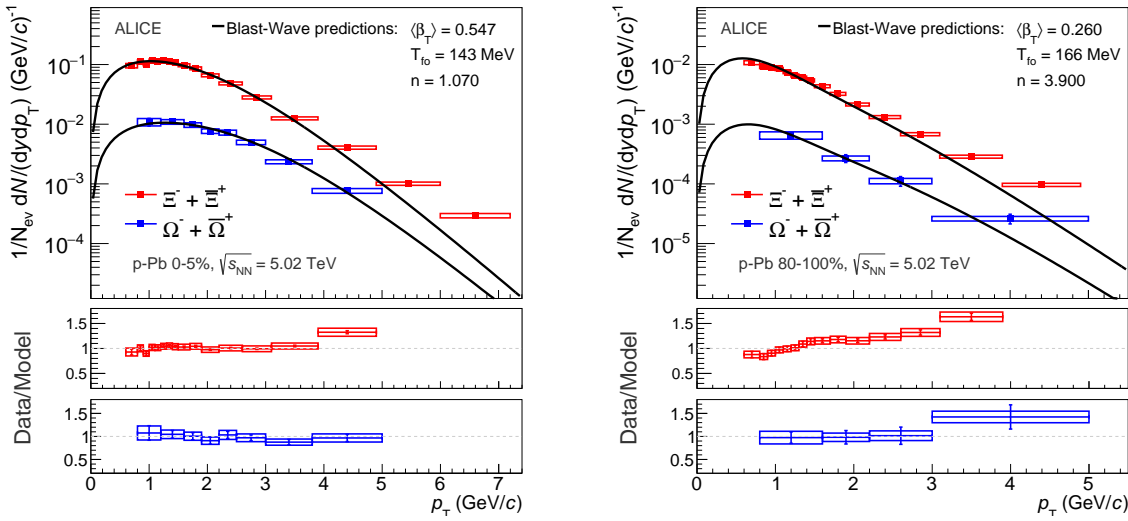


Fig. 3: (colour online) ($\Xi^- + \Xi^+$) and ($\Omega^- + \Omega^+$) p_T spectra in the 0–5% (left) and 80–100% (right) multiplicity classes compared to predictions from the BG-BW model (upper panels) with the ratios on a linear scale (lower panels). The parameters are based on simultaneous fits to lighter hadrons [23]. See text for details.

The Ξ^- , Ξ^+ , Ω^- and Ω^+ p_T spectra in the 0–5% and 80–100% multiplicity classes are compared to predictions from the BG-BW model with parameters acquired from a simultaneous fit to π^\pm , K^\pm , $p(\bar{p})$ and $\Lambda(\bar{\Lambda})$ [23] in Fig. 3. The model describes the measured shapes within uncertainties up to a p_T of approximately 4 GeV/c for Ξ and 5 GeV/c for Ω in the highest multiplicity class. This indicates that multi-strange hadrons also follow a common motion with the lighter hadrons and is suggestive of the presence of radial flow in p–Pb collisions. However, it is worth noting that some final state effects could also modify the spectra in a similar manner to radial flow. For example, PYTHIA [30] implements the colour reconnection mechanism, which fuses strings originating from independent parton interactions, leading to fewer but more energetic hadrons, which has been shown to mimic radial flow [31].

Applying the same technique to results from the lower multiplicity classes reveals that the agreement of the data with the Blast-Wave predictions become progressively worse. The comparison between lowest and highest multiplicity cases can be seen in Fig. 3, where their respective ratios to the model predictions are shown in the lower panels. These observations indicate that common kinetic freeze-out conditions are able to better describe the spectra in high multiplicity p–Pb collisions.

The multi-strange baryon spectra in central Pb–Pb collisions [10] have also been investigated in a common freeze-out scenario [17, 18] and similar studies were performed for Au–Au collisions [19]. In contrast to high multiplicity p–Pb collisions, where all stable and long-lived hadron spectra are compatible with a single set of kinetic freeze-out conditions (the temperature T_{fo} and the mean transverse flow velocity $\langle \beta_T \rangle$), multi-strange particles in central heavy-ion collisions seem to experience less transverse flow and may freeze out earlier in the evolution of the system when compared to most of the other hadrons.

3.3 Hyperon to pion ratios

The measured integrated yields in the seven multiplicity classes are given in Table 3. To study the relative production of strangeness and compare it with results in pp and Pb–Pb collisions, the yield ratios to pions were calculated as a function of charged particle multiplicity. Both the $(\Xi^- + \Xi^+)/(\pi^+ + \pi^-)$ and $(\Omega^- + \Omega^+)/(\pi^+ + \pi^-)$ ratios are observed to increase as a function of multiplicity, as seen in Fig. 4.

Event class	$\langle dN_{\text{ch}}/d\eta \rangle_{ \eta_{\text{lab}} < 0.5}$	$dN/dy(\Xi^- + \bar{\Xi}^+)$	$dN/dy(\Omega^- + \bar{\Omega}^+)$
0–5%	45 ± 1	$0.2354 \pm 0.0020 \pm 0.0161$	$0.0260 \pm 0.0011 \pm 0.0034$
5–10%	36.2 ± 0.8	$0.1861 \pm 0.0016 \pm 0.0138$	$0.0215 \pm 0.0008 \pm 0.0029$
10–20%	30.5 ± 0.7	$0.1500 \pm 0.0010 \pm 0.0112$	$0.0167 \pm 0.0006 \pm 0.0022$
20–40%	23.2 ± 0.5	$0.1100 \pm 0.0006 \pm 0.0085$	$0.0120 \pm 0.0005 \pm 0.0016$
40–60%	16.1 ± 0.4	$0.0726 \pm 0.0006 \pm 0.0065$	$0.0072 \pm 0.0003 \pm 0.0010$
60–80%	9.8 ± 0.2	$0.0398 \pm 0.0004 \pm 0.0031$	$0.0042 \pm 0.0002 \pm 0.0006$
80–100%	4.3 ± 0.1	$0.0143 \pm 0.0003 \pm 0.0015$	$0.0013 \pm 0.0003 \pm 0.0003$

Table 3: The mid-rapidity $\langle dN_{\text{ch}}/d\eta \rangle$ values for each of the 7 multiplicity classes and the $\Xi^- + \bar{\Xi}^+$ and $\Omega^- + \bar{\Omega}^+$ integrated yields per unit rapidity normalised to the visible cross section. The statistical uncertainty on the yields is followed by the systematic uncertainty.

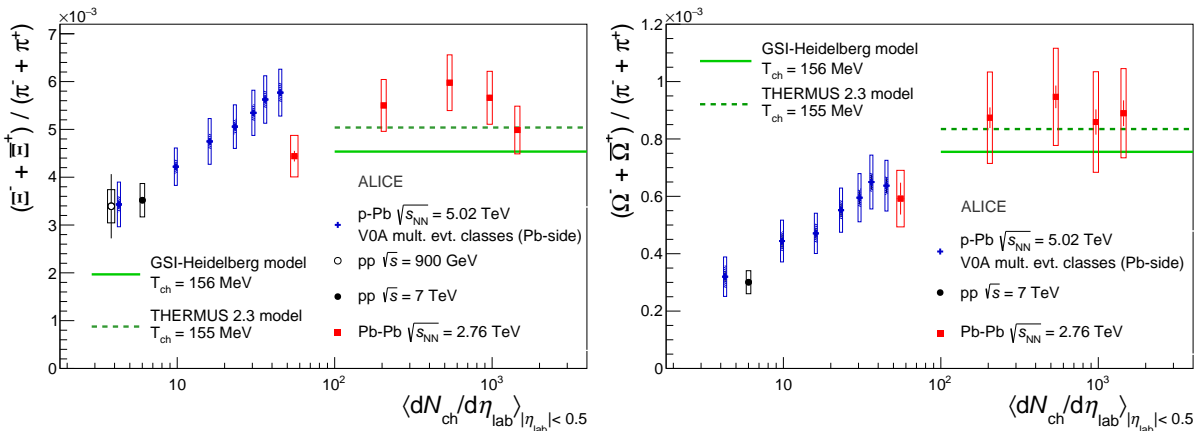


Fig. 4: (colour online) $(\Xi^- + \bar{\Xi}^+)/(\pi^+ + \pi^-)$ (left) and $(\Omega^- + \bar{\Omega}^+)/(\pi^+ + \pi^-)$ (right) ratios as a function of $\langle dN_{\text{ch}}/d\eta \rangle$ for all three colliding systems. The ratios for the seven multiplicity classes in p–Pb data lie between the Minimum Bias pp ($\sqrt{s} = 900$ GeV [32, 33] and $\sqrt{s} = 7$ TeV [25, 34]) and peripheral Pb–Pb results. The Pb–Pb points [10] represent, from left to right, the 60–80%, 40–60%, 20–40% and 10–20% and 0–10% centrality classes. The chemical equilibrium predictions by the GSI-Heidelberg [35] and the THERMUS 2.3 [36] models are represented by the horizontal lines.

The relative increase is more pronounced for the Ω^- and $\bar{\Omega}^+$ than for Ξ^- and $\bar{\Xi}^+$, being approximately 100% for the former and 60% for the latter. These relative increases are larger than the 30% increase observed for the Λ/π ratio [23], indicating that strangeness content may control the rate of increase with multiplicity.

These ratios are further compared to measurements performed in the pp [25, 34] and Pb–Pb [10] collision systems. The $(\Xi^- + \bar{\Xi}^+)/(\pi^+ + \pi^-)$ ratio for the highest p–Pb multiplicity is compatible with the Pb–Pb measurements in the Pb–Pb 0–60% centrality range and the $(\Omega^- + \bar{\Omega}^+)/(\pi^+ + \pi^-)$ reaches a value slightly below its Pb–Pb equivalent in this centrality range, although the error bars still overlap. It is also noteworthy that the values obtained for the p–Pb 80–100% multiplicity event class are similar to the ones measured in minimum bias pp collisions.

Finally, the hyperon to pion ratios can also be compared with the values in the Grand Canonical (GC) limit obtained from global fits to Pb–Pb data. Two different implementations of the thermal model are

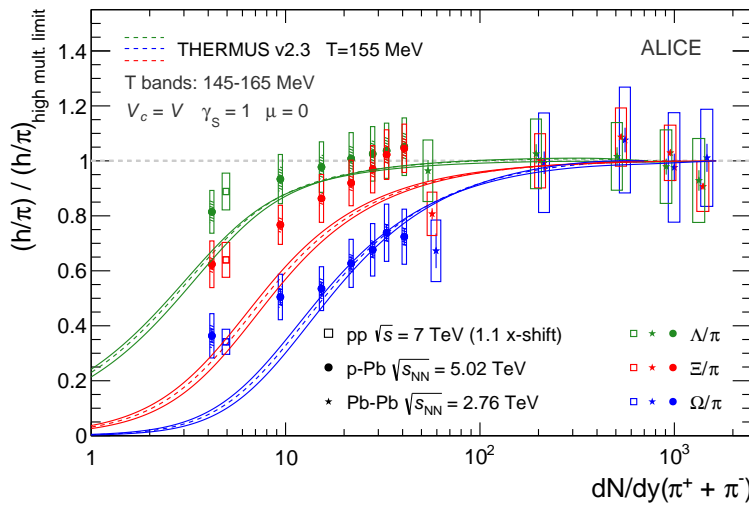


Fig. 5: (colour online) Hyperon to pion ratios as a function of pion yields for pp, p–Pb and Pb–Pb colliding systems compared to the THERMUS [36] strangeness suppression model prediction, in which only the system size is varied. The h/π are the ratios of the particle and antiparticle sums, except for the $2\Lambda/(\pi^- + \pi^+)$ data points in pp [33], p–Pb [23] and Pb–Pb [37]. All values are normalised to the high multiplicity limit, which is given by the mean of the 0–60% highest multiplicity Pb–Pb measurements for the data and by the GC limit for the model.

shown in Fig. 4, where the dashed lines represent the values from the THERMUS 2.3 model [36] and the solid lines represent predictions from the GSI-Heidelberg model [35]. Both models provide values that are consistent with the most central Pb–Pb measurements.

In small multiplicity environments such as those produced in p–Pb collisions, a grand canonical statistical description may not be appropriate. Instead, local conservation laws might play an important role. The evolution of hyperon to pion ratios in terms of the event multiplicity can be calculated with a Strangeness Canonical (SC) model implemented in THERMUS [36]. This model applies a local conservation law to the strangeness quantum number within a correlation volume V_c while treating the baryon and charge quantum numbers grand-canonically within the fireball volume V . This implies a decrease of the strangeness yields with respect to the pion yields with a shrinking system size. To model this canonical suppression effect as a function of pion rapidity density, yield calculations were repeated for varying system sizes. Strangeness conservation was imposed within the size of the fireball ($V_c = V$), and the strangeness saturation parameter γ_s was fixed to 1, thus changes in the hadron to pion ratios were due to the variations of the restraints on the system size only. The chemical potentials (μ) of the conserved strangeness, baryon and electric charge quantum numbers were set to zero. The obtained suppression curves for Λ , Ξ and Ω are shown in Fig. 5 for a temperature of 155 MeV, the value extracted from a GC global fit to high multiplicity Pb–Pb data, with a variation of ± 10 MeV (solid lines). Both the data and model points were normalised to the high multiplicity limit. For the data, this limit is the mean hyperon to pion ratio in the 0–60% most central Pb–Pb events, whereas for the model it corresponds to the GC limit. The theoretical curves for strangeness suppression computed with THERMUS are in qualitative agreement with the effect observed in the data.

4 Conclusions

In summary, a measurement of the p_T spectra of Ξ^- , $\bar{\Xi}^+$, Ω^- and $\bar{\Omega}^+$ for seven multiplicity classes in p–Pb collisions at $\sqrt{s_{\text{NN}}} = 5.02$ TeV at the LHC has been presented. These measurements represent an important contribution to the understanding of strangeness production, as hyperon production rates are

now measured at LHC energies over a large range in charged-particle multiplicity, from pp to central Pb–Pb collisions.

The multi-strange baryon spectra exhibit a progressive flattening with increasing multiplicity suggesting the presence of radial flow. A comparison with the Boltzmann-Gibbs Blast-Wave model indicates a common kinetic freeze-out with lighter hadrons in the highest multiplicity p–Pb collisions. This is in contrast to higher multiplicity heavy-ion collisions where there is an indication for an earlier freeze-out of these particles.

For the first time, the lifting of strangeness suppression with system size has been observed with measurements in a single collision system. Hyperon to pion ratios are shown to increase with multiplicity in p–Pb collisions from the values measured in pp to those observed in Pb–Pb. The rate of increase is more pronounced for particles with higher strangeness content. Comparing these results to the trends observed in statistical hadronisation models that conserve strangeness across the created system indicates that the behaviour is qualitatively consistent with the lifting of canonical suppression with increasing multiplicity.

Acknowledgements

The ALICE Collaboration would like to thank all its engineers and technicians for their invaluable contributions to the construction of the experiment and the CERN accelerator teams for the outstanding performance of the LHC complex. The ALICE Collaboration gratefully acknowledges the resources and support provided by all Grid centres and the Worldwide LHC Computing Grid (WLCG) collaboration. The ALICE Collaboration acknowledges the following funding agencies for their support in building and running the ALICE detector: State Committee of Science, World Federation of Scientists (WFS) and Swiss Fonds Kidagan, Armenia; Conselho Nacional de Desenvolvimento Científico e Tecnológico (CNPq), Financiadora de Estudos e Projetos (FINEP), Fundação de Amparo à Pesquisa do Estado de São Paulo (FAPESP); National Natural Science Foundation of China (NSFC), the Chinese Ministry of Education (CMOE) and the Ministry of Science and Technology of China (MSTC); Ministry of Education and Youth of the Czech Republic; Danish Natural Science Research Council, the Carlsberg Foundation and the Danish National Research Foundation; The European Research Council under the European Community’s Seventh Framework Programme; Helsinki Institute of Physics and the Academy of Finland; French CNRS-IN2P3, the ‘Region Pays de Loire’, ‘Region Alsace’, ‘Region Auvergne’ and CEA, France; German Bundesministerium für Bildung, Wissenschaft, Forschung und Technologie (BMBF) and the Helmholtz Association; General Secretariat for Research and Technology, Ministry of Development, Greece; National Research, Development and Innovation Office (NKFIH), Hungary; Department of Atomic Energy and Department of Science and Technology of the Government of India; Istituto Nazionale di Fisica Nucleare (INFN) and Centro Fermi - Museo Storico della Fisica e Centro Studi e Ricerche “Enrico Fermi”, Italy; Japan Society for the Promotion of Science (JSPS) KAKENHI and MEXT, Japan; Joint Institute for Nuclear Research, Dubna; National Research Foundation of Korea (NRF); Consejo Nacional de Ciencia y Tecnología (CONACYT), Dirección General de Asuntos del Personal Académico (DGAPA), México, Amerique Latine Formation académique - European Commission (ALFA-EC) and the EPLANET Program (European Particle Physics Latin American Network); Stichting voor Fundamenteel Onderzoek der Materie (FOM) and the Nederlandse Organisatie voor Wetenschappelijk Onderzoek (NWO), Netherlands; Research Council of Norway (NFR); National Science Centre, Poland; Ministry of National Education/Institute for Atomic Physics and National Council of Scientific Research in Higher Education (CNCSI-UEFISCDI), Romania; Ministry of Education and Science of Russian Federation, Russian Academy of Sciences, Russian Federal Agency of Atomic Energy, Russian Federal Agency for Science and Innovations and The Russian Foundation for Basic Research; Ministry of Education of Slovakia; Department of Science and Technology, South Africa; Centro de Investigaciones Energeticas, Medioambientales y Tecnologicas (CIEMAT), E-Infrastructure shared

between Europe and Latin America (EELA), Ministerio de Economía y Competitividad (MINECO) of Spain, Xunta de Galicia (Consellería de Educación), Centro de Aplicaciones Tecnológicas y Desarrollo Nuclear (CEADEN), Cubaenergía, Cuba, and IAEA (International Atomic Energy Agency); Swedish Research Council (VR) and Knut & Alice Wallenberg Foundation (KAW); Ukraine Ministry of Education and Science; United Kingdom Science and Technology Facilities Council (STFC); The United States Department of Energy, the United States National Science Foundation, the State of Texas, and the State of Ohio; Ministry of Science, Education and Sports of Croatia and Unity through Knowledge Fund, Croatia; Council of Scientific and Industrial Research (CSIR), New Delhi, India; Pontificia Universidad Católica del Perú.

References

- [1] J. Rafelski and B. Müller, “Strangeness production in the quark-gluon plasma,” *Phys. Rev. Lett.* **48** (1982) 1066–1069. <http://link.aps.org/doi/10.1103/PhysRevLett.48.1066>. [Erratum *Phys. Rev. Lett.* **56** (1986) 2334–2334].
- [2] **WA97** Collaboration, E. Andersen *et al.*, “Enhancement of central Λ , Ξ and Ω yields in Pb-Pb collisions at 158 A GeV/c,” *Physics Letters B* **433** (1998) 209 – 216. <http://www.sciencedirect.com/science/article/pii/S0370269398006893>.
- [3] **WA97** Collaboration, E. Andersen *et al.*, “Strangeness enhancement at mid-rapidity in Pb–Pb collisions at 158 A GeV/c,” *Physics Letters B* **449** (1999) 401 – 406. <http://www.sciencedirect.com/science/article/pii/S0370269399001409>.
- [4] **NA49** Collaboration, S. Afanasiev *et al.*, “ Ξ^- and $\bar{\Xi}^+$ production in central Pb+Pb collisions at 158 GeV/c per nucleon,” *Physics Letters B* **538** (2002) 275 – 281. <http://www.sciencedirect.com/science/article/pii/S0370269302019706>.
- [5] **NA57** Collaboration, F. Antinori *et al.*, “Energy dependence of hyperon production in nucleus–nucleus collisions at SPS,” *Physics Letters B* **595** (2004) 68 – 74. <http://www.sciencedirect.com/science/article/pii/S0370269304007725>.
- [6] **NA49** Collaboration, T. Anticic *et al.*, “ Λ and $\bar{\Lambda}$ production in central Pb-Pb collisions at 40, 80, and 158A GeV,” *Phys. Rev. Lett.* **93** (2004) 022302. <http://link.aps.org/doi/10.1103/PhysRevLett.93.022302>.
- [7] **STAR** Collaboration, J. Adams *et al.*, “Multistrange baryon production in Au-Au collisions at $\sqrt{s_{NN}} = 130$ GeV,” *Phys. Rev. Lett.* **92** (2004) 182301. <http://link.aps.org/doi/10.1103/PhysRevLett.92.182301>.
- [8] **STAR** Collaboration, J. Adams *et al.*, “Scaling properties of hyperon production in Au + Au collisions at $\sqrt{s_{NN}} = 200$ GeV,” *Phys. Rev. Lett.* **98** (2007) 062301. <http://link.aps.org/doi/10.1103/PhysRevLett.98.062301>.
- [9] **STAR** Collaboration, B. I. Abelev *et al.*, “Enhanced strange baryon production in Au+Au collisions compared to $p + p$ at $\sqrt{s_{NN}} = 200$ GeV,” *Phys. Rev. C* **77** (2008) 044908. <http://link.aps.org/doi/10.1103/PhysRevC.77.044908>.
- [10] **ALICE** Collaboration, B. Abelev *et al.*, “Multi-strange baryon production at mid-rapidity in Pb–Pb collisions at $\sqrt{s_{NN}} = 2.76$ TeV,” *Physics Letters B* **728** (2014) 216 – 227. <http://www.sciencedirect.com/science/article/pii/S0370269313009544>.
- [11] K. Redlich and A. Tounsi, “Strangeness enhancement and energy dependence in heavy ion collisions,” *The European Physical Journal C* **24** (2002) 589–594. <http://link.springer.com/article/10.1007/s10052-002-0983-1>.

- [12] I. Kraus, J. Cleymans, H. Oeschler, and K. Redlich, “Particle production in p-p collisions and predictions for $\sqrt{s} = 14$ TeV at the CERN Large Hadron Collider (LHC),” *Phys. Rev. C* **79** (2009) 014901. <http://link.aps.org/doi/10.1103/PhysRevC.79.014901>.
- [13] F. Becattini and J. Manninen, “Strangeness production from SPS to LHC,” *Journal of Physics G: Nuclear and Particle Physics* **35** (2008) 104013. <http://stacks.iop.org/0954-3899/35/i=10/a=104013>.
- [14] J. Aichelin and K. Werner, “Centrality Dependence of Strangeness Enhancement in Ultrarelativistic Heavy Ion Collisions: A Core–Corona Effect,” *Phys. Rev. C* **79** (2009) 064907, arXiv:0810.4465 [nucl-th]. <http://link.aps.org/doi/10.1103/PhysRevC.79.064907>. [Erratum: *Phys. Rev. C* **81**, 029902(2010)].
- [15] **STAR** Collaboration, G. Agakishiev *et al.*, “Strangeness enhancement in Cu-Cu and Au-Au collisions at $\sqrt{s_{\text{NN}}} = 200$ GeV,” *Phys. Rev. Lett.* **108** (2012) 072301. <http://link.aps.org/doi/10.1103/PhysRevLett.108.072301>.
- [16] E. Schnedermann, J. Sollfrank, and U. W. Heinz, “Thermal phenomenology of hadrons from 200A GeV S+S collisions,” *Phys. Rev. C* **48** (1993) 2462–2475, arXiv:nucl-th/9307020 [nucl-th]. <http://link.aps.org/doi/10.1103/PhysRevC.48.2462>.
- [17] V. Begun, W. Florkowski, and M. Rybczynski, “Transverse-momentum spectra of strange particles produced in Pb + Pb collisions at $\sqrt{s_{\text{NN}}} = 2.76$ TeV in the chemical nonequilibrium model,” *Phys. Rev. C* **90** (2014) 054912. <http://link.aps.org/doi/10.1103/PhysRevC.90.054912>.
- [18] I. Melo and B. Tomasik, “Blast wave fits with resonances to p_t spectra from nuclear collisions at the LHC,” in *15th International Conference on Strangeness in Quark Matter (SQM 2015) Dubna, Moscow region, Russia, July 6–11, 2015*. 2015. arXiv:1509.05383 [nucl-th].
- [19] **STAR** Collaboration, J. Adams *et al.*, “Experimental and theoretical challenges in the search for the quark–gluon plasma: The STAR collaboration’s critical assessment of the evidence from RHIC collisions,” *Nuclear Physics A* **757** (2005) 102–183, arXiv:nucl-ex/0501009 [nucl-ex]. <http://www.sciencedirect.com/science/article/pii/S0375947405005294>.
- [20] **ALICE** Collaboration, “The ALICE experiment at the CERN LHC,” *Journal of Instrumentation* **3** (2008) S08002. <http://stacks.iop.org/1748-0221/3/i=08/a=S08002>.
- [21] **ALICE** Collaboration, “Performance of the ALICE VZERO system,” *Journal of Instrumentation* **8** (2013) P10016. <http://stacks.iop.org/1748-0221/8/i=10/a=P10016>.
- [22] **ALICE** Collaboration, B. Abelev *et al.*, “Pseudorapidity density of charged particles in $p + \text{Pb}$ collisions at $\sqrt{s_{\text{NN}}} = 5.02$ TeV,” *Phys. Rev. Lett.* **110** (2013) 032301. <http://link.aps.org/doi/10.1103/PhysRevLett.110.032301>.
- [23] **ALICE** Collaboration, J. Adam *et al.*, “Multiplicity dependence of pion, kaon, proton and lambda production in p-Pb collisions at $\sqrt{s_{\text{NN}}} = 5.02$ TeV,” *Physics Letters B* **728** (2014) 25–38. <http://www.sciencedirect.com/science/article/pii/S0370269313009234>.
- [24] Olive, K.A. *et al.* (Particle Data Group), *Chinese Physics C* **38**, 090001 (2014). <http://stacks.iop.org/1674-1137/38/i=9/a=090001>.
- [25] **ALICE** Collaboration, B. Abelev *et al.*, “Multi-strange baryon production in pp collisions at $\sqrt{s} = 7$ TeV with ALICE,” *Physics Letters B* **712** (2012) 309–318. <http://www.sciencedirect.com/science/article/pii/S037026931200528X>.

- [26] ALICE Collaboration, “Performance of the ALICE experiment at the CERN LHC,” *International Journal of Modern Physics A* **29** (2014) 1430044.
<http://www.worldscientific.com/doi/abs/10.1142/S0217751X14300440>.
- [27] S. Roesler, R. Engel, and J. Ranft, “The Monte Carlo event generator DPMJET-III,” in *Advanced Monte Carlo for Radiation Physics, Particle Transport Simulation and Applications*, A. Kling, F. Barão, M. Nakagawa, L. Távora, and P. Vaz, eds., pp. 1033–1038. Springer Berlin Heidelberg, 2001. arXiv:hep-ph/0012252 [hep-ph].
http://dx.doi.org/10.1007/978-3-642-18211-2_166.
- [28] R. Brun, F. Carminati, and S. Giani, “GEANT Detector Description and Simulation Tool.”.
- [29] C. Tsallis, “Possible Generalization of Boltzmann-Gibbs Statistics,” *J. Statist. Phys.* **52** (1988) 479–487.
- [30] T. Sjostrand, S. Mrenna, and P. Z. Skands, “PYTHIA 6.4 Physics and Manual,” *JHEP* **05** (2006) 026, arXiv:hep-ph/0603175 [hep-ph].
- [31] A. Ortiz Velasquez, P. Christiansen, E. Cuautle Flores, I. A. Maldonado Cervantes, and G. Paić, “Color reconnection and flowlike patterns in pp collisions,” *Phys. Rev. Lett.* **111** (2013) 042001.
<http://link.aps.org/doi/10.1103/PhysRevLett.111.042001>.
- [32] ALICE Collaboration, K. Aamodt *et al.*, “Production of pions, kaons and protons in pp collisions at $\sqrt{s} = 900$ GeV with ALICE at the LHC,” *The European Physical Journal C* **71** (2011) 1655.
<http://dx.doi.org/10.1140/epjc/s10052-011-1655-9>.
- [33] ALICE Collaboration, K. Aamodt *et al.*, “Strange particle production in proton-proton collisions at $\sqrt{s} = 0.9$ TeV with ALICE at the LHC,” *The European Physical Journal C* **71** (2011) 1594.
<http://dx.doi.org/10.1140/epjc/s10052-011-1594-5>.
- [34] ALICE Collaboration, J. Adam *et al.*, “Measurement of pion, kaon and proton production in proton–proton collisions at $\sqrt{s} = 7$ TeV,” *The European Physical Journal C* **75** (2015) 226.
<http://dx.doi.org/10.1140/epjc/s10052-015-3422-9>.
- [35] A. Andronic, P. Braun-Munzinger, and J. Stachel, “Thermal hadron production in relativistic nuclear collisions: The hadron mass spectrum, the horn, and the QCD phase transition,” *Physics Letters B* **673** (2009) 142–145.
<http://www.sciencedirect.com/science/article/pii/S0370269309001609>.
- [36] S. Wheaton, J. Cleymans, and M. Hauer, “THERMUS — a thermal model package for ROOT,” *Computer Physics Communications* **180** (2009) 84 – 106.
<http://www.sciencedirect.com/science/article/pii/S0010465508002750>.
- [37] ALICE Collaboration, B. B. Abelev *et al.*, “ K_S^0 and Λ production in Pb-Pb collisions at $\sqrt{s_{NN}} = 2.76$ TeV,” *Phys. Rev. Lett.* **111** (2013) 222301, arXiv:1307.5530 [nucl-ex].

A The ALICE Collaboration

J. Adam⁴⁰, D. Adamová⁸⁴, M.M. Aggarwal⁸⁸, G. Aglieri Rinella³⁶, M. Agnello¹¹⁰, N. Agrawal⁴⁸, Z. Ahammed¹³², S. Ahmad¹⁹, S.U. Ahn⁶⁸, S. Aiola¹³⁶, A. Akindinov⁵⁸, S.N. Alam¹³², D. Aleksandrov⁸⁰, B. Alessandro¹¹⁰, D. Alexandre¹⁰¹, R. Alfaro Molina⁶⁴, A. Alici^{12,104}, A. Alkin³, J.R.M. Almaraz¹¹⁹, J. Alme³⁸, T. Alt⁴³, S. Altinpinar¹⁸, I. Altsybeev¹³¹, C. Alves Garcia Prado¹²⁰, C. Andrei⁷⁸, A. Andronic⁹⁷, V. Anguelov⁹⁴, J. Anielski⁵⁴, T. Antičić⁹⁸, F. Antinori¹⁰⁷, P. Antonioli¹⁰⁴, L. Aphecetche¹¹³, H. Appelhäuser⁵³, S. Arcelli²⁸, R. Arnaldi¹¹⁰, O.W. Arnold^{37,93}, I.C. Arsene²², M. Arslandok⁵³, B. Audurier¹¹³, A. Augustinus³⁶, R. Averbeck⁹⁷, M.D. Azmi¹⁹, A. Badalà¹⁰⁶, Y.W. Baek⁶⁷, S. Bagnasco¹¹⁰, R. Bailhache⁵³, R. Bala⁹¹, S. Balasubramanian¹³⁶, A. Baldissari¹⁵, R.C. Baral⁶¹, A.M. Barbano²⁷, R. Barbera²⁹, F. Barile³³, G.G. Barnaföldi¹³⁵, L.S. Barnby¹⁰¹, V. Barret⁷⁰, P. Bartalini⁷, K. Barth³⁶, J. Bartke¹¹⁷, E. Bartsch⁵³, M. Basile²⁸, N. Bastid⁷⁰, S. Basu¹³², B. Bathen⁵⁴, G. Batigne¹¹³, A. Batista Camejo⁷⁰, B. Batyunya⁶⁶, P.C. Batzing²², I.G. Bearden⁸¹, H. Beck⁵³, C. Bedda¹¹⁰, N.K. Behera⁵⁰, I. Belikov⁵⁵, F. Bellini²⁸, H. Bello Martinez², R. Bellwied¹²², R. Belmont¹³⁴, E. Belmont-Moreno⁶⁴, V. Belyaev⁷⁵, P. Benacek⁸⁴, G. Bencedi¹³⁵, S. Beole²⁷, I. Berceanu⁷⁸, A. Bercuci⁷⁸, Y. Berdnikov⁸⁶, D. Berenyi¹³⁵, R.A. Bertens⁵⁷, D. Berzana³⁶, L. Betev³⁶, A. Bhasin⁹¹, I.R. Bhat⁹¹, A.K. Bhati⁸⁸, B. Bhattacharjee⁴⁵, J. Bhom¹²⁸, L. Bianchi¹²², N. Bianchi⁷², C. Bianchin^{134,57}, J. Bielčík⁴⁰, J. Bielčíková⁸⁴, A. Bilandžić^{81,37,93}, G. Biro¹³⁵, R. Biswas⁴, S. Biswas⁷⁹, S. Bjelogrlic⁵⁷, J.T. Blair¹¹⁸, D. Blau⁸⁰, C. Blume⁵³, F. Bock^{74,94}, A. Bogdanov⁷⁵, H. Bøggild⁸¹, L. Boldizsár¹³⁵, M. Bombara⁴¹, J. Bok⁵³, H. Borel¹⁵, A. Borissov⁹⁶, M. Borri^{83,124}, F. Bossú⁶⁵, E. Botta²⁷, C. Bourjau⁸¹, P. Braun-Munzinger⁹⁷, M. Bregant¹²⁰, T. Breitner⁵², T.A. Broker⁵³, T.A. Browning⁹⁵, M. Broz⁴⁰, E.J. Brucken⁴⁶, E. Bruna¹¹⁰, G.E. Bruno³³, D. Budnikov⁹⁹, H. Buesching⁵³, S. Bufalino^{36,27}, P. Buncic³⁶, O. Busch^{94,128}, Z. Buthelezi⁶⁵, J.B. Butt¹⁶, J.T. Buxton²⁰, D. Caffarri³⁶, X. Cai⁷, H. Caines¹³⁶, L. Calero Diaz⁷², A. Caliva⁵⁷, E. Calvo Villar¹⁰², P. Camerini²⁶, F. Carena³⁶, W. Carena³⁶, F. Carnesecchi²⁸, J. Castillo Castellanos¹⁵, A.J. Castro¹²⁵, E.A.R. Casula²⁵, C. Ceballos Sanchez⁹, P. Cerello¹¹⁰, J. Cerkala¹¹⁵, B. Chang¹²³, S. Chapeland³⁶, M. Chartier¹²⁴, J.L. Charvet¹⁵, S. Chattopadhyay¹³², S. Chattopadhyay¹⁰⁰, A. Chauvin^{93,37}, V. Chelnokov³, M. Cherney⁸⁷, C. Cheshkov¹³⁰, B. Cheynis¹³⁰, V. Chibante Barroso³⁶, D.D. Chinellato¹²¹, S. Cho⁵⁰, P. Chochula³⁶, K. Choi⁹⁶, M. Chojnacki⁸¹, S. Choudhury¹³², P. Christakoglou⁸², C.H. Christensen⁸¹, P. Christiansen³⁴, T. Chujo¹²⁸, S.U. Chung⁹⁶, C. Cicalo¹⁰⁵, L. Cifarelli^{12,28}, F. Cindolo¹⁰⁴, J. Cleymans⁹⁰, F. Colamaria³³, D. Colella^{59,36}, A. Collu^{74,25}, M. Colocci²⁸, G. Conesa Balbastre⁷¹, Z. Conesa del Valle⁵¹, M.E. Connors^{ii,136}, J.G. Contreras⁴⁰, T.M. Cormier⁸⁵, Y. Corrales Morales¹¹⁰, I. Cortés Maldonado², P. Cortese³², M.R. Cosentino¹²⁰, F. Costa³⁶, P. Crochet⁷⁰, R. Cruz Albino¹¹, E. Cuautle⁶³, L. Cunqueiro^{54,36}, T. Dahms^{93,37}, A. Dainese¹⁰⁷, A. Danu⁶², D. Das¹⁰⁰, I. Das^{100,51}, S. Das⁴, A. Dash^{121,79}, S. Dash⁴⁸, S. De¹²⁰, A. De Caro^{12,31}, G. de Cataldo¹⁰³, C. de Conti¹²⁰, J. de Cuveland⁴³, A. De Falco²⁵, D. De Gruttola^{12,31}, N. De Marco¹¹⁰, S. De Pasquale³¹, A. Deisting^{97,94}, A. Deloff⁷⁷, E. Dénes^{135,i}, C. Deplano⁸², P. Dhankher⁴⁸, D. Di Bari³³, A. Di Mauro³⁶, P. Di Nezza⁷², M.A. Diaz Corchero¹⁰, T. Dietel⁹⁰, P. Dillenseger⁵³, R. Divia³⁶, Ø. Djupsland¹⁸, A. Dobrin^{57,82}, D. Domenicis Gimenez¹²⁰, B. Dönigus⁵³, O. Dordic²², T. Drozhzhova⁵³, A.K. Dubey¹³², A. Dubla⁵⁷, L. Ducroux¹³⁰, P. Dupieux⁷⁰, R.J. Ehlers¹³⁶, D. Elia¹⁰³, E. Endress¹⁰², H. Engel⁵², E. Epple¹³⁶, B. Erazmus¹¹³, I. Erdemir⁵³, F. Erhardt¹²⁹, B. Espagnon⁵¹, M. Estienne¹¹³, S. Esumi¹²⁸, J. Eum⁹⁶, D. Evans¹⁰¹, S. Evdokimov¹¹¹, G. Eyyubova⁴⁰, L. Fabbietti^{93,37}, D. Fabris¹⁰⁷, J. Faivre⁷¹, A. Fantoni⁷², M. Fasel⁷⁴, L. Feldkamp⁵⁴, A. Feliciello¹¹⁰, G. Feofilov¹³¹, J. Ferencei⁸⁴, A. Fernández Téllez², E.G. Ferreiro¹⁷, A. Ferretti²⁷, A. Festanti³⁰, V.J.G. Feuillard^{15,70}, J. Figiel¹¹⁷, M.A.S. Figueiredo^{124,120}, S. Filchagin⁹⁹, D. Finogeev⁵⁶, F.M. Fionda²⁵, E.M. Fiore³³, M.G. Fleck⁹⁴, M. Floris³⁶, S. Foertsch⁶⁵, P. Foka⁹⁷, S. Fokin⁸⁰, E. Fragiacomo¹⁰⁹, A. Francescon^{36,30}, U. Frankenfeld⁹⁷, G.G. Fronze²⁷, U. Fuchs³⁶, C. Furget⁷¹, A. Furs⁵⁶, M. Fusco Girard³¹, J.J. Gaardhøje⁸¹, M. Gagliardi²⁷, A.M. Gago¹⁰², M. Gallio²⁷, D.R. Gangadharan⁷⁴, P. Ganoti⁸⁹, C. Gao⁷, C. Garabatos⁹⁷, E. Garcia-Solis¹³, C. Gargiulo³⁶, P. Gasik^{93,37}, E.F. Gauger¹¹⁸, M. Germain¹¹³, A. Gheata³⁶, M. Gheata^{36,62}, P. Ghosh¹³², S.K. Ghosh⁴, P. Gianotti⁷², P. Giubellino^{110,36}, P. Giubilato³⁰, E. Gladysz-Dziadus¹¹⁷, P. Glässel⁹⁴, D.M. Goméz Coral⁶⁴, A. Gomez Ramirez⁵², V. Gonzalez¹⁰, P. González-Zamora¹⁰, S. Gorbunov⁴³, L. Görlich¹¹⁷, S. Gotovac¹¹⁶, V. Grabski⁶⁴, O.A. Grachov¹³⁶, L.K. Graczykowski¹³³, K.L. Graham¹⁰¹, A. Grelli⁵⁷, A. Grigoras³⁶, C. Grigoras³⁶, V. Grigoriev⁷⁵, A. Grigoryan¹, S. Grigoryan⁶⁶, B. Grinyov³, N. Grion¹⁰⁹, J.M. Gronefeld⁹⁷, J.F. Grosse-Oetringhaus³⁶, J.-Y. Grossiord¹³⁰, R. Grossiord⁹⁷, F. Guber⁵⁶, R. Guernane⁷¹, B. Guerzoni²⁸, K. Gulbrandsen⁸¹, T. Gunji¹²⁷, A. Gupta⁹¹, R. Gupta⁹¹, R. Haake⁵⁴, Ø. Haaland¹⁸, C. Hadjidakis⁵¹, M. Haiduc⁶², H. Hamagaki¹²⁷, G. Hamar¹³⁵, J.C. Hamon⁵⁵, J.W. Harris¹³⁶, A. Harton¹³, D. Hatzifotiadou¹⁰⁴, S. Hayashi¹²⁷, S.T. Heckel⁵³, H. Helstrup³⁸, A. Herghelegiu⁷⁸, G. Herrera Corral¹¹, B.A. Hess³⁵, K.F. Hetland³⁸, H. Hillemanns³⁶, B. Hippolyte⁵⁵, D. Horak⁴⁰, R. Hosokawa¹²⁸, P. Hristov³⁶, M. Huang¹⁸, T.J. Humanic²⁰, N. Hussain⁴⁵, T. Hussain¹⁹,

D. Hutter⁴³, D.S. Hwang²¹, R. Ilkaev⁹⁹, M. Inaba¹²⁸, E. Incani²⁵, M. Ippolitov^{75,80}, M. Irfan¹⁹, M. Ivanov⁹⁷, V. Ivanov⁸⁶, V. Izucheev¹¹¹, N. Jacazio²⁸, P.M. Jacobs⁷⁴, M.B. Jadhav⁴⁸, S. Jadlovska¹¹⁵, J. Jadlovsky^{115,59}, C. Jahnke¹²⁰, M.J. Jakubowska¹³³, H.J. Jang⁶⁸, M.A. Janik¹³³, P.H.S.Y. Jayarathna¹²², C. Jena³⁰, S. Jena¹²², R.T. Jimenez Bustamante⁹⁷, P.G. Jones¹⁰¹, H. Jung⁴⁴, A. Jusko¹⁰¹, P. Kalinak⁵⁹, A. Kalweit³⁶, J. Kamin⁵³, J.H. Kang¹³⁷, V. Kaplin⁷⁵, S. Kar¹³², A. Karasu Uysal⁶⁹, O. Karavichev⁵⁶, T. Karavicheva⁵⁶, L. Karayan^{97,94}, E. Karpechev⁵⁶, U. Kebschull⁵², R. Keidel¹³⁸, D.L.D. Keijdener⁵⁷, M. Keil³⁶, M. Mohisin Khan^{iii,19}, P. Khan¹⁰⁰, S.A. Khan¹³², A. Khanzadeev⁸⁶, Y. Kharlov¹¹¹, B. Kileng³⁸, D.W. Kim⁴⁴, D.J. Kim¹²³, D. Kim¹³⁷, H. Kim¹³⁷, J.S. Kim⁴⁴, M. Kim⁴⁴, M. Kim¹³⁷, S. Kim²¹, T. Kim¹³⁷, S. Kirsch⁴³, I. Kisel⁴³, S. Kiselev⁵⁸, A. Kisiel¹³³, G. Kiss¹³⁵, J.L. Klay⁶, C. Klein⁵³, J. Klein³⁶, C. Klein-Bösing⁵⁴, S. Klewin⁹⁴, A. Kluge³⁶, M.L. Knichel⁹⁴, A.G. Knospe¹¹⁸, C. Kobdaj¹¹⁴, M. Kofarago³⁶, T. Kollegger⁹⁷, A. Kolojvari¹³¹, V. Kondratiev¹³¹, N. Kondratyeva⁷⁵, E. Kondratyuk¹¹¹, A. Konevskikh⁵⁶, M. Kopcik¹¹⁵, M. Kour⁹¹, C. Kouzinopoulos³⁶, O. Kovalenko⁷⁷, V. Kovalenko¹³¹, M. Kowalski¹¹⁷, G. Koyithatta Meethaleveedu⁴⁸, I. Králik⁵⁹, A. Kravčáková⁴¹, M. Kretz⁴³, M. Krivda^{59,101}, F. Krizek⁸⁴, E. Kryshen^{86,36}, M. Krzewicki⁴³, A.M. Kubera²⁰, V. Kučera⁸⁴, C. Kuhn⁵⁵, P.G. Kuijer⁸², A. Kumar⁹¹, J. Kumar⁴⁸, L. Kumar⁸⁸, S. Kumar⁴⁸, P. Kurashvili⁷⁷, A. Kurepin⁵⁶, A.B. Kurepin⁵⁶, A. Kuryakin⁹⁹, M.J. Kweon⁵⁰, Y. Kwon¹³⁷, S.L. La Pointe¹¹⁰, P. La Rocca²⁹, P. Ladron de Guevara¹¹, C. Lagana Fernandes¹²⁰, I. Lakomov³⁶, R. Langoy⁴², C. Lara⁵², A. Lardeux¹⁵, A. Lattuca²⁷, E. Laudi³⁶, R. Lea²⁶, L. Leardini⁹⁴, G.R. Lee¹⁰¹, S. Lee¹³⁷, F. Lehas⁸², R.C. Lemmon⁸³, V. Lenti¹⁰³, E. Leogrande⁵⁷, I. León Monzón¹¹⁹, H. León Vargas⁶⁴, M. Leoncino²⁷, P. Lévai¹³⁵, S. Li^{7,70}, X. Li¹⁴, J. Lien⁴², R. Lietava¹⁰¹, S. Lindal²², V. Lindenstruth⁴³, C. Lippmann⁹⁷, M.A. Lisa²⁰, H.M. Ljunggren³⁴, D.F. Lodato⁵⁷, P.I. Loenne¹⁸, V. Loginov⁷⁵, C. Loizides⁷⁴, X. Lopez⁷⁰, E. López Torres⁹, A. Lowe¹³⁵, P. Luettig⁵³, M. Lunardon³⁰, G. Luparello²⁶, T.H. Lutz¹³⁶, A. Maevskaya⁵⁶, M. Mager³⁶, S. Mahajan⁹¹, S.M. Mahmood²², A. Maire⁵⁵, R.D. Majka¹³⁶, M. Malaev⁸⁶, I. Maldonado Cervantes⁶³, L. Malinina^{iv,66}, D. Mal'Kevich⁵⁸, P. Malzacher⁹⁷, A. Mamontov⁹⁹, V. Manko⁸⁰, F. Manso⁷⁰, V. Manzari^{36,103}, M. Marchisone^{65,126,27}, J. Mareš⁶⁰, G.V. Margagliotti²⁶, A. Margotti¹⁰⁴, J. Margutti⁵⁷, A. Marín⁹⁷, C. Markert¹¹⁸, M. Marquard⁵³, N.A. Martin⁹⁷, J. Martin Blanco¹¹³, P. Martinengo³⁶, M.I. Martínez², G. Martínez García¹¹³, M. Martinez Pedreira³⁶, A. Mas¹²⁰, S. Masciocchi⁹⁷, M. Masera²⁷, A. Masoni¹⁰⁵, L. Massacrier¹¹³, A. Mastrosorio³³, A. Matyja¹¹⁷, C. Mayer^{36,117}, J. Mazer¹²⁵, M.A. Mazzoni¹⁰⁸, D. McDonald¹²², F. Meddi²⁴, Y. Melikyan⁷⁵, A. Menchaca-Rocha⁶⁴, E. Meninno³¹, J. Mercado Pérez⁹⁴, M. Meres³⁹, Y. Miake¹²⁸, M.M. Mieskolainen⁴⁶, K. Mikhaylov^{66,58}, L. Milano^{74,36}, J. Milosevic²², L.M. Minervini^{103,23}, A. Mischke⁵⁷, A.N. Mishra⁴⁹, D. Miśkowiec⁹⁷, J. Mitra¹³², C.M. Mitu⁶², N. Mohammadi⁵⁷, B. Mohanty^{79,132}, L. Molnar^{55,113}, L. Montaño Zetina¹¹, E. Montes¹⁰, D.A. Moreira De Godoy^{54,113}, L.A.P. Moreno², S. Moretto³⁰, A. Morreale¹¹³, A. Morsch³⁶, V. Muccifora⁷², E. Mudnic¹¹⁶, D. Mühlheim⁵⁴, S. Muhuri¹³², M. Mukherjee¹³², J.D. Mulligan¹³⁶, M.G. Munhoz¹²⁰, R.H. Munzer^{93,37}, H. Murakami¹²⁷, S. Murray⁶⁵, L. Musa³⁶, J. Musinsky⁵⁹, B. Naik⁴⁸, R. Nair⁷⁷, B.K. Nandi⁴⁸, R. Nania¹⁰⁴, E. Nappi¹⁰³, M.U. Naru¹⁶, H. Natal da Luz¹²⁰, C. Natrass¹²⁵, S.R. Navarro², K. Nayak⁷⁹, R. Nayak⁴⁸, T.K. Nayak¹³², S. Nazarenko⁹⁹, A. Nedosekin⁵⁸, L. Nellen⁶³, F. Ng¹²², M. Nicassio⁹⁷, M. Niculescu⁶², J. Niedziela³⁶, B.S. Nielsen⁸¹, S. Nikolaev⁸⁰, S. Nikulin⁸⁰, V. Nikulin⁸⁶, F. Noferini^{104,12}, P. Nomokonov⁶⁶, G. Nooren⁵⁷, J.C.C. Noris², J. Norman¹²⁴, A. Nyanin⁸⁰, J. Nystrand¹⁸, H. Oeschler⁹⁴, S. Oh¹³⁶, S.K. Oh⁶⁷, A. Ohlson³⁶, A. Okatan⁶⁹, T. Okubo⁴⁷, L. Olah¹³⁵, J. Oleniacz¹³³, A.C. Oliveira Da Silva¹²⁰, M.H. Oliver¹³⁶, J. Onderwaater⁹⁷, C. Oppedisano¹¹⁰, R. Orava⁴⁶, A. Ortiz Velasquez⁶³, A. Oskarsson³⁴, J. Otwinowski¹¹⁷, K. Oyama^{94,76}, M. Ozdemir⁵³, Y. Pachmayer⁹⁴, P. Pagano³¹, G. Paic⁶³, S.K. Pal¹³², J. Pan¹³⁴, A.K. Pandey⁴⁸, P. Papcun¹¹⁵, V. Papikyan¹, G.S. Pappalardo¹⁰⁶, P. Pareek⁴⁹, W.J. Park⁹⁷, S. Parmar⁸⁸, A. Passfeld⁵⁴, V. Paticchio¹⁰³, R.N. Patra¹³², B. Paul¹⁰⁰, H. Pei⁷, T. Peitzmann⁵⁷, H. Pereira Da Costa¹⁵, D. Peresunko^{80,75}, C.E. Pérez Lara⁸², E. Perez Lezama⁵³, V. Peskov⁵³, Y. Pestov⁵, V. Petráček⁴⁰, V. Petrov¹¹¹, M. Petrovici⁷⁸, C. Petta²⁹, S. Piano¹⁰⁹, M. Pikna³⁹, P. Pillot¹¹³, L.O.D.L. Pimentel⁸¹, O. Pinazza^{36,104}, L. Pinsky¹²², D.B. Piyarathna¹²², M. Płoskoń⁷⁴, M. Planinic¹²⁹, J. Pluta¹³³, S. Pochybova¹³⁵, P.L.M. Podesta-Lerma¹¹⁹, M.G. Poghosyan^{85,87}, B. Polichtchouk¹¹¹, N. Poljak¹²⁹, W. Poonsawat¹¹⁴, A. Pop⁷⁸, S. Porteboeuf-Houssais⁷⁰, J. Porter⁷⁴, J. Pospisil⁸⁴, S.K. Prasad⁴, R. Preghenella^{104,36}, F. Prino¹¹⁰, C.A. Pruneau¹³⁴, I. Pshenichnov⁵⁶, M. Puccio²⁷, G. Puddu²⁵, P. Pujahari¹³⁴, V. Punin⁹⁹, J. Putschke¹³⁴, H. Qvigstad²², A. Rachevski¹⁰⁹, S. Raha⁴, S. Rajput⁹¹, J. Rak¹²³, A. Rakotozafindrabe¹⁵, L. Ramello³², F. Rami⁵⁵, R. Raniwala⁹², S. Raniwala⁹², S.S. Räsänen⁴⁶, B.T. Rascanu⁵³, D. Rathee⁸⁸, K.F. Read^{125,85}, K. Redlich⁷⁷, R.J. Reed¹³⁴, A. Rehman¹⁸, P. Reichelt⁵³, F. Reidt^{94,36}, X. Ren⁷, R. Renfordt⁵³, A.R. Reolon⁷², A. Reshetin⁵⁶, J.-P. Revol¹², K. Reygers⁹⁴, V. Riabov⁸⁶, R.A. Ricci⁷³, T. Richert³⁴, M. Richter²², P. Riedler³⁶, W. Riegler³⁶, F. Riggi²⁹, C. Ristea⁶², E. Rocco⁵⁷, M. Rodríguez Cahuantzi^{2,11}, A. Rodriguez Manso⁸², K. Røed²², E. Rogochaya⁶⁶, D. Rohr⁴³, D. Röhrich¹⁸, R. Romita¹²⁴, F. Ronchetti^{72,36}, L. Ronflette¹¹³, P. Rosnet⁷⁰, A. Rossi^{30,36}, F. Roukoutakis⁸⁹, A. Roy⁴⁹,

C. Roy⁵⁵, P. Roy¹⁰⁰, A.J. Rubio Montero¹⁰, R. Rui²⁶, R. Russo²⁷, E. Ryabinkin⁸⁰, Y. Ryabov⁸⁶, A. Rybicki¹¹⁷, S. Sadovsky¹¹¹, K. Šafařík³⁶, B. Sahlmuller⁵³, P. Sahoo⁴⁹, R. Sahoo⁴⁹, S. Sahoo⁶¹, P.K. Sahu⁶¹, J. Saini¹³², S. Sakai⁷², M.A. Saleh¹³⁴, J. Salzwedel²⁰, S. Sambyal⁹¹, V. Samsonov⁸⁶, L. Šádor⁵⁹, A. Sandoval⁶⁴, M. Sano¹²⁸, D. Sarkar¹³², P. Sarma⁴⁵, E. Scapparone¹⁰⁴, F. Scarlassara³⁰, C. Schiaua⁷⁸, R. Schicker⁹⁴, C. Schmidt⁹⁷, H.R. Schmidt³⁵, S. Schuchmann⁵³, J. Schukraft³⁶, M. Schulc⁴⁰, T. Schuster¹³⁶, Y. Schutz^{36,113}, K. Schwarz⁹⁷, K. Schweda⁹⁷, G. Scioli²⁸, E. Scomparin¹¹⁰, R. Scott¹²⁵, M. Šefčík⁴¹, J.E. Seger⁸⁷, Y. Sekiguchi¹²⁷, D. Sekihata⁴⁷, I. Selyuzhenkov⁹⁷, K. Senosi⁶⁵, S. Senyukov^{3,36}, E. Serradilla^{10,64}, A. Sevcenco⁶², A. Shabanov⁵⁶, A. Shabetai¹¹³, O. Shadura³, R. Shahoyan³⁶, A. Shangaraev¹¹¹, A. Sharma⁹¹, M. Sharma⁹¹, M. Sharma⁹¹, N. Sharma¹²⁵, K. Shigaki⁴⁷, K. Shtejer^{9,27}, Y. Sibiriak⁸⁰, S. Siddhanta¹⁰⁵, K.M. Sielewicz³⁶, T. Siemianczuk⁷⁷, D. Silvermyr³⁴, C. Silvestre⁷¹, G. Simatovic¹²⁹, G. Simonetti³⁶, R. Singaraju¹³², R. Singh⁷⁹, S. Singha^{132,79}, V. Singhal¹³², B.C. Sinha¹³², T. Sinha¹⁰⁰, B. Sitar³⁹, M. Sitta³², T.B. Skaali²², M. Slupecki¹²³, N. Smirnov¹³⁶, R.J.M. Snellings⁵⁷, T.W. Snellman¹²³, C. Søgaard³⁴, J. Song⁹⁶, M. Song¹³⁷, Z. Song⁷, F. Soramel³⁰, S. Sorensen¹²⁵, R.D. de Souza¹²¹, F. Sozzi⁹⁷, M. Spacek⁴⁰, E. Spiriti⁷², I. Sputowska¹¹⁷, M. Spyropoulou-Stassinaki⁸⁹, J. Stachel⁹⁴, I. Stan⁶², P. Stankus⁸⁵, G. Stefanek⁷⁷, E. Stenlund³⁴, G. Steyn⁶⁵, J.H. Stiller⁹⁴, D. Stocco¹¹³, P. Strmen³⁹, A.A.P. Suaide¹²⁰, T. Sugitate⁴⁷, C. Suire⁵¹, M. Suleymanov¹⁶, M. Suljic^{26,i}, R. Sultanov⁵⁸, M. Šumbera⁸⁴, A. Szabo³⁹, A. Szanto de Toledo^{120,i}, I. Szarka³⁹, A. Szczepankiewicz³⁶, M. Szymanski¹³³, U. Tabassam¹⁶, J. Takahashi¹²¹, G.J. Tambave¹⁸, N. Tanaka¹²⁸, M.A. Tangaro³³, M. Tarhini⁵¹, M. Tariq¹⁹, M.G. Tarzila⁷⁸, A. Tauro³⁶, G. Tejeda Muñoz², A. Telesca³⁶, K. Terasaki¹²⁷, C. Terrevoli³⁰, B. Teyssier¹³⁰, J. Thäder⁷⁴, D. Thomas¹¹⁸, R. Tieulent¹³⁰, A.R. Timmins¹²², A. Toia⁵³, S. Trogolo²⁷, G. Trombetta³³, V. Trubnikov³, W.H. Trzaska¹²³, T. Tsuji¹²⁷, A. Tumkin⁹⁹, R. Turrisi¹⁰⁷, T.S. Tveter²², K. Ullaland¹⁸, A. Uras¹³⁰, G.L. Usai²⁵, A. Utrobicic¹²⁹, M. Vajzer⁸⁴, M. Vala⁵⁹, L. Valencia Palomo⁷⁰, S. Vallero²⁷, J. Van Der Maarel⁵⁷, J.W. Van Hoorn³⁶, M. van Leeuwen⁵⁷, T. Vanat⁸⁴, P. Vande Vyvre³⁶, D. Varga¹³⁵, A. Vargas², M. Vargyas¹²³, R. Varma⁴⁸, M. Vasileiou⁸⁹, A. Vasiliev⁸⁰, A. Vauthier⁷¹, V. Vechernin¹³¹, A.M. Veen⁵⁷, M. Veldhoen⁵⁷, A. Velure¹⁸, M. Venaruzzo⁷³, E. Vercellin²⁷, S. Vergara Limón², R. Vernet⁸, M. Verweij¹³⁴, L. Vickovic¹¹⁶, G. Viesti^{30,i}, J. Viinikainen¹²³, Z. Vilakazi¹²⁶, O. Villalobos Baillie¹⁰¹, A. Villatoro Tello², A. Vinogradov⁸⁰, L. Vinogradov¹³¹, Y. Vinogradov^{99,i}, T. Virgili³¹, V. Vislavicius³⁴, Y.P. Viyogi¹³², A. Vodopyanov⁶⁶, M.A. Völkl⁹⁴, K. Voloshin⁵⁸, S.A. Voloshin¹³⁴, G. Volpe¹³⁵, B. von Haller³⁶, I. Vorobyev^{37,93}, D. Vranic^{97,36}, J. Vrláková⁴¹, B. Vulpescu⁷⁰, B. Wagner¹⁸, J. Wagner⁹⁷, H. Wang⁵⁷, M. Wang^{7,113}, D. Watanabe¹²⁸, Y. Watanabe¹²⁷, M. Weber^{36,112}, S.G. Weber⁹⁷, D.F. Weiser⁹⁴, J.P. Wessels⁵⁴, U. Westerhoff⁵⁴, A.M. Whitehead⁹⁰, J. Wiechula³⁵, J. Wikne²², M. Wilde⁵⁴, G. Wilk⁷⁷, J. Wilkinson⁹⁴, M.C.S. Williams¹⁰⁴, B. Windelband⁹⁴, M. Winn⁹⁴, C.G. Yaldo¹³⁴, H. Yang⁵⁷, P. Yang⁷, S. Yano⁴⁷, C. Yasar⁶⁹, Z. Yin⁷, H. Yokoyama¹²⁸, I.-K. Yoo⁹⁶, J.H. Yoon⁵⁰, V. Yurchenko³, I. Yushmanov⁸⁰, A. Zaborowska¹³³, V. Zaccolo⁸¹, A. Zaman¹⁶, C. Zampolli¹⁰⁴, H.J.C. Zanolli¹²⁰, S. Zaporozhets⁶⁶, N. Zardoshti¹⁰¹, A. Zarochentsev¹³¹, P. Závada⁶⁰, N. Zaviyalov⁹⁹, H. Zbroszczyk¹³³, I.S. Zgura⁶², M. Zhalov⁸⁶, H. Zhang¹⁸, X. Zhang⁷⁴, Y. Zhang⁷, C. Zhang⁵⁷, Z. Zhang⁷, C. Zhao²², N. Zhigareva⁵⁸, D. Zhou⁷, Y. Zhou⁸¹, Z. Zhou¹⁸, H. Zhu¹⁸, J. Zhu^{113,7}, A. Zichichi^{28,12}, A. Zimmermann⁹⁴, M.B. Zimmermann^{54,36}, G. Zinovjev³, M. Zyzak⁴³

Affiliation notes

ⁱ Deceased

ⁱⁱ Also at: Georgia State University, Atlanta, Georgia, United States

ⁱⁱⁱ Also at: Also at Department of Applied Physics, Aligarh Muslim University, Aligarh, India

^{iv} Also at: M.V. Lomonosov Moscow State University, D.V. Skobeltsyn Institute of Nuclear, Physics, Moscow, Russia

Collaboration Institutes

¹ A.I. Alikhanyan National Science Laboratory (Yerevan Physics Institute) Foundation, Yerevan, Armenia

² Benemérita Universidad Autónoma de Puebla, Puebla, Mexico

³ Bogolyubov Institute for Theoretical Physics, Kiev, Ukraine

⁴ Bose Institute, Department of Physics and Centre for Astroparticle Physics and Space Science (CAPSS), Kolkata, India

⁵ Budker Institute for Nuclear Physics, Novosibirsk, Russia

⁶ California Polytechnic State University, San Luis Obispo, California, United States

⁷ Central China Normal University, Wuhan, China

- ⁸ Centre de Calcul de l'IN2P3, Villeurbanne, France
⁹ Centro de Aplicaciones Tecnológicas y Desarrollo Nuclear (CEADEN), Havana, Cuba
¹⁰ Centro de Investigaciones Energéticas Medioambientales y Tecnológicas (CIEMAT), Madrid, Spain
¹¹ Centro de Investigación y de Estudios Avanzados (CINVESTAV), Mexico City and Mérida, Mexico
¹² Centro Fermi - Museo Storico della Fisica e Centro Studi e Ricerche "Enrico Fermi", Rome, Italy
¹³ Chicago State University, Chicago, Illinois, USA
¹⁴ China Institute of Atomic Energy, Beijing, China
¹⁵ Commissariat à l'Energie Atomique, IRFU, Saclay, France
¹⁶ COMSATS Institute of Information Technology (CIIT), Islamabad, Pakistan
¹⁷ Departamento de Física de Partículas and IGFAE, Universidad de Santiago de Compostela, Santiago de Compostela, Spain
¹⁸ Department of Physics and Technology, University of Bergen, Bergen, Norway
¹⁹ Department of Physics, Aligarh Muslim University, Aligarh, India
²⁰ Department of Physics, Ohio State University, Columbus, Ohio, United States
²¹ Department of Physics, Sejong University, Seoul, South Korea
²² Department of Physics, University of Oslo, Oslo, Norway
²³ Dipartimento di Elettrotecnica ed Elettronica del Politecnico, Bari, Italy
²⁴ Dipartimento di Fisica dell'Università 'La Sapienza' and Sezione INFN Rome, Italy
²⁵ Dipartimento di Fisica dell'Università and Sezione INFN, Cagliari, Italy
²⁶ Dipartimento di Fisica dell'Università and Sezione INFN, Trieste, Italy
²⁷ Dipartimento di Fisica dell'Università and Sezione INFN, Turin, Italy
²⁸ Dipartimento di Fisica e Astronomia dell'Università and Sezione INFN, Bologna, Italy
²⁹ Dipartimento di Fisica e Astronomia dell'Università and Sezione INFN, Catania, Italy
³⁰ Dipartimento di Fisica e Astronomia dell'Università and Sezione INFN, Padova, Italy
³¹ Dipartimento di Fisica 'E.R. Caianiello' dell'Università and Gruppo Collegato INFN, Salerno, Italy
³² Dipartimento di Scienze e Innovazione Tecnologica dell'Università del Piemonte Orientale and Gruppo Collegato INFN, Alessandria, Italy
³³ Dipartimento Interateneo di Fisica 'M. Merlin' and Sezione INFN, Bari, Italy
³⁴ Division of Experimental High Energy Physics, University of Lund, Lund, Sweden
³⁵ Eberhard Karls Universität Tübingen, Tübingen, Germany
³⁶ European Organization for Nuclear Research (CERN), Geneva, Switzerland
³⁷ Excellence Cluster Universe, Technische Universität München, Munich, Germany
³⁸ Faculty of Engineering, Bergen University College, Bergen, Norway
³⁹ Faculty of Mathematics, Physics and Informatics, Comenius University, Bratislava, Slovakia
⁴⁰ Faculty of Nuclear Sciences and Physical Engineering, Czech Technical University in Prague, Prague, Czech Republic
⁴¹ Faculty of Science, P.J. Šafárik University, Košice, Slovakia
⁴² Faculty of Technology, Buskerud and Vestfold University College, Vestfold, Norway
⁴³ Frankfurt Institute for Advanced Studies, Johann Wolfgang Goethe-Universität Frankfurt, Frankfurt, Germany
⁴⁴ Gangneung-Wonju National University, Gangneung, South Korea
⁴⁵ Gauhati University, Department of Physics, Guwahati, India
⁴⁶ Helsinki Institute of Physics (HIP), Helsinki, Finland
⁴⁷ Hiroshima University, Hiroshima, Japan
⁴⁸ Indian Institute of Technology Bombay (IIT), Mumbai, India
⁴⁹ Indian Institute of Technology Indore, Indore (IITI), India
⁵⁰ Inha University, Incheon, South Korea
⁵¹ Institut de Physique Nucléaire d'Orsay (IPNO), Université Paris-Sud, CNRS-IN2P3, Orsay, France
⁵² Institut für Informatik, Johann Wolfgang Goethe-Universität Frankfurt, Frankfurt, Germany
⁵³ Institut für Kernphysik, Johann Wolfgang Goethe-Universität Frankfurt, Frankfurt, Germany
⁵⁴ Institut für Kernphysik, Westfälische Wilhelms-Universität Münster, Münster, Germany
⁵⁵ Institut Pluridisciplinaire Hubert Curien (IPHC), Université de Strasbourg, CNRS-IN2P3, Strasbourg, France
⁵⁶ Institute for Nuclear Research, Academy of Sciences, Moscow, Russia
⁵⁷ Institute for Subatomic Physics of Utrecht University, Utrecht, Netherlands
⁵⁸ Institute for Theoretical and Experimental Physics, Moscow, Russia

- ⁵⁹ Institute of Experimental Physics, Slovak Academy of Sciences, Košice, Slovakia
⁶⁰ Institute of Physics, Academy of Sciences of the Czech Republic, Prague, Czech Republic
⁶¹ Institute of Physics, Bhubaneswar, India
⁶² Institute of Space Science (ISS), Bucharest, Romania
⁶³ Instituto de Ciencias Nucleares, Universidad Nacional Autónoma de México, Mexico City, Mexico
⁶⁴ Instituto de Física, Universidad Nacional Autónoma de México, Mexico City, Mexico
⁶⁵ iThemba LABS, National Research Foundation, Somerset West, South Africa
⁶⁶ Joint Institute for Nuclear Research (JINR), Dubna, Russia
⁶⁷ Konkuk University, Seoul, South Korea
⁶⁸ Korea Institute of Science and Technology Information, Daejeon, South Korea
⁶⁹ KTO Karatay University, Konya, Turkey
⁷⁰ Laboratoire de Physique Corpusculaire (LPC), Clermont Université, Université Blaise Pascal, CNRS-IN2P3, Clermont-Ferrand, France
⁷¹ Laboratoire de Physique Subatomique et de Cosmologie, Université Grenoble-Alpes, CNRS-IN2P3, Grenoble, France
⁷² Laboratori Nazionali di Frascati, INFN, Frascati, Italy
⁷³ Laboratori Nazionali di Legnaro, INFN, Legnaro, Italy
⁷⁴ Lawrence Berkeley National Laboratory, Berkeley, California, United States
⁷⁵ Moscow Engineering Physics Institute, Moscow, Russia
⁷⁶ Nagasaki Institute of Applied Science, Nagasaki, Japan
⁷⁷ National Centre for Nuclear Studies, Warsaw, Poland
⁷⁸ National Institute for Physics and Nuclear Engineering, Bucharest, Romania
⁷⁹ National Institute of Science Education and Research, Bhubaneswar, India
⁸⁰ National Research Centre Kurchatov Institute, Moscow, Russia
⁸¹ Niels Bohr Institute, University of Copenhagen, Copenhagen, Denmark
⁸² Nikhef, Nationaal instituut voor subatomaire fysica, Amsterdam, Netherlands
⁸³ Nuclear Physics Group, STFC Daresbury Laboratory, Daresbury, United Kingdom
⁸⁴ Nuclear Physics Institute, Academy of Sciences of the Czech Republic, Řež u Prahy, Czech Republic
⁸⁵ Oak Ridge National Laboratory, Oak Ridge, Tennessee, United States
⁸⁶ Petersburg Nuclear Physics Institute, Gatchina, Russia
⁸⁷ Physics Department, Creighton University, Omaha, Nebraska, United States
⁸⁸ Physics Department, Panjab University, Chandigarh, India
⁸⁹ Physics Department, University of Athens, Athens, Greece
⁹⁰ Physics Department, University of Cape Town, Cape Town, South Africa
⁹¹ Physics Department, University of Jammu, Jammu, India
⁹² Physics Department, University of Rajasthan, Jaipur, India
⁹³ Physik Department, Technische Universität München, Munich, Germany
⁹⁴ Physikalisches Institut, Ruprecht-Karls-Universität Heidelberg, Heidelberg, Germany
⁹⁵ Purdue University, West Lafayette, Indiana, United States
⁹⁶ Pusan National University, Pusan, South Korea
⁹⁷ Research Division and ExtreMe Matter Institute EMMI, GSI Helmholtzzentrum für Schwerionenforschung, Darmstadt, Germany
⁹⁸ Rudjer Bošković Institute, Zagreb, Croatia
⁹⁹ Russian Federal Nuclear Center (VNIIEF), Sarov, Russia
¹⁰⁰ Saha Institute of Nuclear Physics, Kolkata, India
¹⁰¹ School of Physics and Astronomy, University of Birmingham, Birmingham, United Kingdom
¹⁰² Sección Física, Departamento de Ciencias, Pontificia Universidad Católica del Perú, Lima, Peru
¹⁰³ Sezione INFN, Bari, Italy
¹⁰⁴ Sezione INFN, Bologna, Italy
¹⁰⁵ Sezione INFN, Cagliari, Italy
¹⁰⁶ Sezione INFN, Catania, Italy
¹⁰⁷ Sezione INFN, Padova, Italy
¹⁰⁸ Sezione INFN, Rome, Italy
¹⁰⁹ Sezione INFN, Trieste, Italy
¹¹⁰ Sezione INFN, Turin, Italy
¹¹¹ SSC IHEP of NRC Kurchatov institute, Protvino, Russia

- ¹¹² Stefan Meyer Institut für Subatomare Physik (SMI), Vienna, Austria
¹¹³ SUBATECH, Ecole des Mines de Nantes, Université de Nantes, CNRS-IN2P3, Nantes, France
¹¹⁴ Suranaree University of Technology, Nakhon Ratchasima, Thailand
¹¹⁵ Technical University of Košice, Košice, Slovakia
¹¹⁶ Technical University of Split FESB, Split, Croatia
¹¹⁷ The Henryk Niewodniczanski Institute of Nuclear Physics, Polish Academy of Sciences, Cracow, Poland
¹¹⁸ The University of Texas at Austin, Physics Department, Austin, Texas, USA
¹¹⁹ Universidad Autónoma de Sinaloa, Culiacán, Mexico
¹²⁰ Universidade de São Paulo (USP), São Paulo, Brazil
¹²¹ Universidade Estadual de Campinas (UNICAMP), Campinas, Brazil
¹²² University of Houston, Houston, Texas, United States
¹²³ University of Jyväskylä, Jyväskylä, Finland
¹²⁴ University of Liverpool, Liverpool, United Kingdom
¹²⁵ University of Tennessee, Knoxville, Tennessee, United States
¹²⁶ University of the Witwatersrand, Johannesburg, South Africa
¹²⁷ University of Tokyo, Tokyo, Japan
¹²⁸ University of Tsukuba, Tsukuba, Japan
¹²⁹ University of Zagreb, Zagreb, Croatia
¹³⁰ Université de Lyon, Université Lyon 1, CNRS/IN2P3, IPN-Lyon, Villeurbanne, France
¹³¹ V. Fock Institute for Physics, St. Petersburg State University, St. Petersburg, Russia
¹³² Variable Energy Cyclotron Centre, Kolkata, India
¹³³ Warsaw University of Technology, Warsaw, Poland
¹³⁴ Wayne State University, Detroit, Michigan, United States
¹³⁵ Wigner Research Centre for Physics, Hungarian Academy of Sciences, Budapest, Hungary
¹³⁶ Yale University, New Haven, Connecticut, United States
¹³⁷ Yonsei University, Seoul, South Korea
¹³⁸ Zentrum für Technologietransfer und Telekommunikation (ZTT), Fachhochschule Worms, Worms, Germany